

# Research Journal of Pharmaceutical, Biological and Chemical Sciences

## Corrosion Inhibition Study Of The *Origanum elongatum* Extract: Electrochemical, Gravimetric And Adsorption Isotherms Studies In 0.5 M Sulfuric Acid.

El Attari Hassan<sup>1\*</sup>, Chefira Khalil<sup>1</sup>, Rchid Halima<sup>2</sup>, Nmila Rachid<sup>2</sup>, Siniti Mustapha<sup>3</sup>, Hanane Oualili<sup>2</sup>, and Houssine Ait Sir<sup>4</sup>.

<sup>1</sup>Departement de Chimie, Laboratoire de Chimie de Coordination et d'Analytique, Université Chouaib Doukkali 24000 El Jadida, Morocco

<sup>2</sup>Departement de Biologie, Equipe Biotechnologies et Valorisation des Ressources Naturelles, Université Chouaib Doukkali 24000 El Jadida, Morocco

<sup>3</sup>Departement de Chimie, Equipe de Thermodynamique, Surfaces et Catalyse, Université Chouaib Doukkali 24000 El Jadida, Morocco.

<sup>4</sup>Departement de Chimie, Laboratoire de Chimie BioOrganique, Université Chouaib Doukkali 24000 El Jadida, Morocco.

### ABSTRACT

Bligh and Dyer extract of an endemic species called *Origanum elongatum* was studied as a corrosion inhibitor in H<sub>2</sub>SO<sub>4</sub> medium at a concentration of 0.5 M by gravimetry method, linear polarization and electrochemical impedance spectroscopy. gravimetry at three different temperatures 25°C, 35°C and 45°C, electrochemical tests were performed at room temperature including linear polarization which shows that this extract acts as a mixed inhibitor, electrochemical parameters were calculated such as E<sub>corr</sub> the anode and cathode slopes  $\beta_a$  and  $\beta_c$ , then electrochemical impedance spectroscopy which shows that the extract forms a protective layer on the metal surface, thermodynamic parameters were calculated and discussed such as free enthalpy, enthalpy and entropy. a confirmation of the type of adsorption by the use of the Dubinin-Radushkevich isotherm, the use of the Bockris-Swinkels isotherm allows to know the number of water molecules displaced by the adsorption of a single active species.

**Keywords:** *Origanum elongatum* extract, Potentiodynamic Polarization Data, Electrochemical Impedance Spectroscopy (EIS), Langmuir isotherm, Dubinin-Radushkevich isotherm, Bockris-Swinkels isotherm.

\*Corresponding author

## INTRODUCTION

Steel is widely used in industry and machinery; on the other hand, it corrodes in aggressive media [1], but also hydrochloric and sulfuric acids are used in the stripping and descaling of mild steel [2], hence the need to use corrosion inhibitors [3,4], organic molecules that contain heteroatoms such as oxygen, nitrogen, sulfur ... are likely to have a stronger corrosion inhibiting effect [5,6], this type of inhibitor has a detrimental effect on the fauna and flora [7], hence the tendency to use molecules of plant origin for their non-toxicity and their availability [8-10].

There are several authors who have worked on plant extracts, A. El Bribri et al worked on a methanolic extract of *Euphorbia falcata L.* in 1M HCl, they are found to be 93.2% effective at a concentration of 3g/L [10], for M. Faustin et al, their work on alkaloids extract from *Geissospermum laeve* in 1M hydrochloric acid, found an efficiency of 92% for a concentration of 100mg/L [11], L. Bammou et al, who studied the efficacy of inhibition of *Chenopodium Ambrosioides* extract in 0.5M H<sub>2</sub>SO<sub>4</sub>, and they found an efficiency of 94% for a concentration of 4g/L [12], Mayakrishnan Prabakaran et al, investigated the inhibition of *Cryptostegia grandiflora* leaf extract was evaluated for its anti-corrosion property on mild steel in 1 M H<sub>2</sub>SO<sub>4</sub>, a maximum efficiency of 87.54% was found for a concentration of 500 ppm [13], pour N. Soltani et al, Their work consisted of testing *Silybum marianum* leaf extract as a 304 stainless steel corrosion inhibitor in a 1 M HCl solution, by gravimetry they found a maximum efficiency of 95.5% for a concentration of 1.2 g/L [14].

Finally this list of examples we will quote the work of S.A. Umoren et al [15] they found that leaf and stem extracts of *Sida acuta* both inhibited corrosion with maximum efficiencies of 85% at a concentration of 0.5 g/L for leaf extract at 30°C and 52% for the extract of stem for a concentration of 0.5g/L at a temperature of 30°C. The plant *Origanum elongatum* was harvested in "Targuist" in the Rif in the north of Morocco (34° 57' North 4° 18' West). The leaves and flowers are dried in the shade in a dry and airy place, the composition of *Origanum elongatum* was cited by the work of Hassan Ramzi et al [16].

## MATERIALS AND METHODS

### EXTRACTION METHOD

The powder of *Origanum elongatum* (leaves and flowers) was extracted with a mixture of methanol / chloroform (2/1; v / v) and with constant stirring. The extracts were evaporated by a rotary evaporator and then reduced to powder by lyophilization.

### WEIGHT LOSS MEASUREMENTS

Carbon steel specimens of the following chemical composition (wt%) were used in the experiment: 0.38 per cent (C), 0.23 per cent (Si), 0.68 per cent (Mn), 0.01 per cent (P), 0.02 per cent (S) and the remainder iron, were used in the studies. Gravimetric method is the most simple and reliable method for the determination of inhibition efficiency. The mild steel sheets of 1cm × 1cm × 0.1 cm were abraded with a series of emery paper (grade 320-500-800) and washed thoroughly with triple distilled water, degreased with acetone and dried using air flow at room temperature. After weighing accurately, the specimens were immersed in 30 mL beaker, which contained 30 mL sulfuric acid with and without addition of different concentrations of extract. After 6 h in different temperature, the specimens were taken out, washed, dried, and weighed accurately. Experiments were carried out in triplicate.

The average weight loss of three parallel mild steel sheets could be obtained. Then the tests were repeated at different temperatures, and mass loss was expressed in g and corrosion rate in g.cm<sup>-2</sup>.h<sup>-1</sup>. The corrosion rate  $C_r$  (g.cm<sup>-2</sup>.h<sup>-1</sup>) is calculated from [17]:

$$C_r = \frac{W_0 - W_t}{S \times t} \quad (1)$$

Where  $W_0$  is the initial weight before immersion,  $W_1$  the final weight after the corrosion test, respectively,  $S$  is the total surface area of specimens,  $t$  is exposure time. The percentage protection efficiency (%E) of extract was calculated by applying the following relation [18]:

$$\% E = \left( 1 - \frac{C_r^I}{C_r^0} \right) \times 100 \quad (2)$$

Where  $C_r^0$  and  $C_r^I$  are the values of corrosion rate without and with inhibitor, respectively.

### ELECTROCHEMICAL MEASUREMENTS

A three-electrode cell was used with a carbon steel (WE) working electrode, a platinum counter electrode (CE) and a saturated calomel reference electrode (SCE). The working electrode (WE) was Covered with an epoxy resin so that it only a working surface of 1 cm<sup>2</sup>. The working area was 1.0 x 1.0 cm<sup>2</sup> and prepared as described above (Weight loss measurements). The electrochemical equipment used is EC-Lab SP 200 Research Gradostat model / galvanostat / FRA. The data were analysed using the EC-Lab software.

The polarization curves were recorded using a three-electrode system. The working electrode was first immersed in the test solution for 30 minutes to establish an open circuit potential ( $E_{ocp}$ ). After measuring the open circuit potential, potentiodynamic polarization curves were obtained with a sweep rate of 1 mV.s<sup>-1</sup> in the potential range between  $\pm 10$  V and  $E_{ocp}$ . The density of the corrosion current ( $j_{corr}$ ) was obtained by extrapolation of the anodic and cathodic Tafel to the corrosion potential. Inhibition Efficiency %E is defined as follows [19]:

$$\% E = \left( 1 - \frac{j_{corr}^{inh}}{j_{corr}^0} \right) \times 100 \quad (3)$$

Where:  $j_{Corr}^0$  and  $j_{Corr}^{inh}$  represent respectively the corrosion current density without and with an inhibitor.

Electrochemical impedance spectroscopy (EIS) was performed at open-circuit potential ( $E_{ocp}$ ) in a frequency range from 100 kHz to 10 MHz, with a signal amplitude perturbation of 10 mV. The inhibition efficiency % E is estimated using the following relationship [20]:

$$\% E = \left( 1 - \frac{R_{ct}^0}{R_{ct}^{inh}} \right) \times 100 \quad (4)$$

Where:  $R_{ct}^0$  and  $R_{ct}^{inh}$ , respectively represent the charge transfer resistance without and with the inhibitor.

## RESULTS AND DISCUSSION

### ELECTROCHEMICAL MEASUREMENTS

#### POTENTIODYNAMIC POLARIZATION DATA

Figure 1 shows the polarization curves of different concentrations of the extract ranging from white to a concentration of 1 g/L in an acid medium (0.5M H<sub>2</sub>SO<sub>4</sub>) at room temperature, the corrosion current density ( $j_{corr}$ ) was calculated from the intersection of Tafel lines.

From Figure 1, we note a displacement of the anodic side of the curves after the addition of different concentrations of the extract, we also note that the addition of a concentration of the extract varies the corrosion potential ( $E_{corr}$ ) decreases ranging from -399.446 mV/ESC to -365.607 mV/ESC, and since this variation does not reach the value of (85 mV) it can be deduced that this inhibitor is of mixed types [18,21] with an anodic tendency but it acts on the dissolution of the metal and on the reaction of the release of hydrogen [22,23] with displacement a slight displacement towards anode potentials. Regarding the corrosion current ( $j_{corr}$ ) according to Table 1, the significant decrease from 31.471  $\mu\text{A}/\text{cm}^2$  to 56.426  $\mu\text{A}/\text{cm}^2$  is noted, it can be seen from Figure 1 that the anodic and cathodic currents decreases significantly during the addition of the extract, which indicates the formation of a protective layer by the adsorbed molecules which block the active sites on the metal surface by reducing the contact area [24].

The effectiveness of the inhibition was calculated by Equation (3) and shown in Table 1, it can be seen that the efficiency increases when the concentration is increased to reach a maximum value of 82.17% for a concentration of 1g/L.

### ELECTROCHEMICAL IMPEDANCE SPECTROSCOPY (EIS)

Figure 2(left) shows the Nyquist plot for different concentrations of OEE in 0.5M  $\text{H}_2\text{SO}_4$ , this figure shows that after the addition of different concentration of the extract the charge transfer resistance ( $R_{ct}$ ) increases this is seen by the increase of the amplitude of the semicircles each time the concentration is increased, according to the representation of Bode Figure 2(right) one also notices that the phase  $\Phi(\text{Deg})$  decreases since one sees a clear difference between that of the white one and that of the other concentrations, and that the  $Z$  modulus decreases when adding OEE extract, it can be seen that in intermediate frequencies there is a linear relationship between the modulus of  $Z$  and the frequency with a slope approaching -1 and a phase angle of almost  $-60^\circ$ , this implies a capacitive behaviour at these frequencies [25], it is recognized that for a perfect capacitive system the shear must reach a value of  $90^\circ$  and a slope -1 [26].

Table 2 represents Electrochemical parameters deduced by EIS method for mild steel in 0.5M $\text{H}_2\text{SO}_4$  in the absence and presence of various concentrations of OEE, these results were found by using an equivalent circuit which is represented in the Figure 3[27], it can be seen that the  $R_{ct}$  value increases with the increase of the concentration of the OEE in the acid to reach a maximum value of 67.47 $\Omega$  for a concentration of 1g/L which corresponds to a maximum effectiveness of 72.70% for this same concentration, this increase in  $R_{ct}$  is often explained by the formation of a protective layer on the metal surface [28], or the reduction of the surface in contact with the solution which makes it possible to delay the process of charge transfer [29].

$C_{dl}$  decreases that can explain the same thing as increasing  $R_{ct}$ [28], but it can also explain the increase in the thickness of the layer forming or the decrease of the local dielectric constant [30] according to Helmholtz's relation [31]:

$$C_{dl} = \frac{\varepsilon \times \varepsilon_0 \times A}{d} \quad (5)$$

Where  $d$  is the thickness of the protective layer,  $\varepsilon$  the dielectric constant of the medium,  $\varepsilon_0$  the vacuum permittivity and  $A$  is the effective surface area of the electrode.

### WEIGHT LOSS STUDIES

The values of the corrosion rate  $Cr$  ( $\text{g}\cdot\text{cm}^{-2}\cdot\text{h}^{-1}$ ), the recovery rate and the efficiency of the % $E$  inhibition obtained by the mass loss method are shown in the Table 3. The value of  $\theta$  was calculated by [32]:

$$\theta = \frac{\%E}{100} \quad (6)$$

From Table 3 It is observed that this compound inhibits the corrosion of mild steel. The inhibition efficiency increases by increasing the concentration of the extract. The increase in the concentration of the extract results in an increase in the part of the metal surface covered by the inhibitory molecules and this leads

to an increase in the inhibition efficiency. Thus, these results reveal the ability of the OEE to act as a protective layer of corrosion on the mild steel and its thickness significantly affects the corrosion protection properties. It is observed that for a concentration of 1 g/L of the extract, the efficiency is about 77.50% at 298K, which shows a very good adsorbability on the surface of the carbon steel.

**ADSORPTION ISOTHERM**

Adsorption isotherms are important means in the knowledge of the information of interactions between steel and the inhibitor [33], there are several types of Langmuir, Flory-Huggins, Frumkin isotherms and others (Table 4). Recovery rates ( $\vartheta$ ) and concentrations ( $C$ ) of OEE are used to represent the different adsorption isotherms. The Table 5 presents the different isotherms and their equations, the values of the parameters  $K_{ads}$ , correlation factor  $R^2$ ....:

The graphical representations of these isotherms are shown in Figure 4, the choice of Modified Langmuir isotherm is based on the value of the slope find which is greater than 1 and that the ordinate at the origin is not zero [34].

From Table 5 we notice that the Langmuir isotherm at the highest correlation factor  $R^2$ , so will be chosen to perform the thermodynamic calculations,

Still according to Table 5, the factor  $x$  of the Flory-Huggins isotherm is positive which shows that the adsorbed species move more than just one molecule of water [30]. The negative value of  $\alpha$  of the Temkin isotherm makes it possible to deduce that there is a repulsion between the adsorbed molecules of the OEE [35,36], the term  $n$  in the Freundlich isotherm formula is between 0 and 1, which means that the adsorption of the OEE molecules is easy [35,37] this value far from the ideal value of 0.6 implies that the process of adsorption does not follow the Freundlich isotherm [34], we can see the formation of a monolayer since  $\gamma < 1$  in the isotherm of El-Awady [38,39], As far as the Adejo-Ekwenchi isotherm is concerned, the parameter  $b$  increases with increasing temperature which implies that a chemisorption [37,40], this conflicts with the previous deductions made with the Langmuir isotherm, the use of another isotherm, such as the Dubinin-Radushkevich isotherm, gives an idea of the nature of the adsorption [41], the parameter  $\alpha$  of the Frumkin isotherm is positive which supposes an attraction within the adsorbed layer [42].

A parameter is often used  $R_L$  called dimensionless separation factor, when the value of  $R_L$  is between 0 and 1 this indicates that the adsorption is favourable but the value is close to 0 plus the adsorption is favourable [43], however when  $R_L$  is greater than 1 adsorption is unfavourable, where  $R_L=0$ , we have an irreversible adsorption [44]. Table 6 presents the different  $R_L$  values calculated from the Langmuir isotherm for the OEE, it can be seen that the  $R_L$  values are all very low approaching the 0, confirming that adsorption of OEE active species is favourable [45,46], very low values are found for all concentrations, indicating that the adsorption is favourable [47].

After choosing Langmuir, a calculation of  $\Delta H_{ads}^0$  and  $\Delta S_{ads}^0$  is necessary, we know that according to El-Attari et al [48]:

$$\Delta G_{ads}^0 = \Delta H_{ads}^0 - (T \times \Delta S_{ads}^0) \quad (7)$$

From Figure 5  $\Delta G_{ads}^0$  vs. temperature, the thermodynamic parameters such as  $\Delta H_{ads}^0$  and  $\Delta S_{ads}^0$  were calculated by the Gibbs-Helmholtz Equation (7); the results are shown in the Table 7.

We can see that the value of standard free energy of adsorption  $\Delta G_{ads}^0$  according to Table 7 it varies between -27.70 and -26.99 kJ/mol, and it is recognized that a value of  $\Delta G_{ads}^0$  at about 20 kJ/mol indicates a phenomenon of physisorption between the molecules of the inhibitor and the metal plate is the case in our study, on the other hand a value of 40 kJ/mol can explain a phenomenon of chemisorption [32,49,50].

And according to Lutendo C. Murulana et al [51] A value of enthalpy of adsorption  $\Delta H_{ads}^0$  around 40 kJ/mol indicates a physisorption in our study this value is -38.195 kJ/mol which confirms the affirmation that the molecules of our OEE act by a physisorption with the metallic surface, And according to D. Ben Hmamou et al [49] a negative value of  $\Delta H_{ads}^0$  indicates an exothermic process [52]. The entropy of adsorption  $\Delta S_{ads}^0$  does not vary but remains negative for all temperatures which may imply an order in the adsorption of the OEE molecules on the metal surface [53].

The use of other isotherms such as Dubinin-Radushkevich makes it possible to distinguish between physisorption and chemisorption [54,55], This model was designed by Dubinin and his colleague for subcritical vapor studies in microporous solids where the adsorption process follows a pore-filling mechanism on an energetically non-uniform surface [56], the Dubinin-Radushkevich isotherm is written under the formulashown in the Figure 6[57,41] :

$$\ln(\theta) = \ln(\theta_{max}) - (a \times \sigma^2) \quad (8)$$

Where  $\theta_{max}$  is the maximum recovery rate,  $\sigma$  (Polany potential) which is:

$$\sigma = R \times T \times \ln\left(1 + \frac{1}{C}\right) \quad (9)$$

C is the concentration of the inhibitor, the parameter a gives the average energy of adsorption E in kJ/mol, which is the energy needed to move one mole of the adsorbate from infinity (solution) to the metal surface, it is written as follows [54]:

$$E = \frac{1}{\sqrt{2 \times a}} \quad (10)$$

It is recognized that the value of E allows to identify the type of adsorption since a value less than 8 kJ/mol, a physisorption exists, while a value greater than or equal to 8 kJ/mol defines a chemisorption [58].

In our case, the value of E is less than 8 kJ/mol (Table 8), which indicates that the adsorption between the adsorbed OEE molecules and the metal surface is a physical adsorption.

The results obtained using Langmuir, Dubinin-Radushkevich and Adejo-Ekwenchi isotherms confirm the existence of both types of adsorption, despite the value of  $\Delta G_{ads}^0$ , this may be due to the existence of several molecules in the extract, molecules that physically adsorb and others chemically [59].

To check the number of molecules of water displaced during the adsorption of the active species in the extract, the Bockris-Swinkels isotherm used by Sylvester O. Adejo et al [35] his formula is [55]:

$$\Delta G_{ads}^0 = -2,303 \times R \times T \times \log \left[ \frac{1000}{C(1-\theta)^n} \times \theta \times \frac{[\theta + (1-\theta)^n]^{n-1}}{n^n} \right] \quad (11)$$

Fouda et al [60] used the term F( $\vartheta$ ) in the equation (12) to determine the number of water molecules replaced, one finds similar work in the work of Mahmoud M. Saleh and Asem A. Atia [61], their calculation is based on the plotting of the log factor F( $\vartheta$ ) as a function of the log(C) of the inhibitor, is to have the number of displaced water molecules the slope must be as close as possible to 1.

$$F(\theta) = \theta \times \frac{[\theta + (1-\theta)^n]^{n-1}}{(1-\theta)^n \times n^n} \quad (12)$$

The Figure 7 shows the Bockris-Swinkels isotherm in different temperatures for the OEE in 0.5M H<sub>2</sub>SO<sub>4</sub>;

It has been found that for a temperature of 298 K the active species or species move between 8 molecules of water since the slopes found are 0.9896, for 308K the active species moves between 4 and 5 water molecules - a slope of 1.0695 for  $n = 5$ -; finally for 318K the active species displaces 3 water molecules adsorbed a slope of 0.9246, these values are identical to those found for the  $1/y$  parameter of the El-Awady isotherm, which confirms the results found since the value of  $1/y$  gives the number of molecules displaced by a molecule of inhibitor adsorbed.

There is confusion about the parameter  $y$  in the El-Awady isotherm, Ali Fathima Sabirneeza Abdul Rahiman and Subhashini Sethumanickam [62] say that a high value of it allows to say that a single active molecule allows to replace 3 to 4 molecules of water, and that a low value of  $1/y$  suggests an adsorbed layer formed of several layers, for Joshua Olusegun Okeniyi [38] a value of  $1/y > 1$  confirms the formation of a multilayer, but for A.S. Fouda et al [63] the value of  $1/y$  represents the number of active sites occupied by a single inhibitory molecule, in our case the value of  $1/y$  in the El-Awady isotherm is the number of water molecules displaced by the adsorption of a single inhibitor molecule.

#### KINETIC/THERMODYNAMICS CONSIDERATIONS

To study the effect of temperature on the adsorption behaviour of the OEE in 0.5M H<sub>2</sub>SO<sub>4</sub>, gravimetric tests were carried out in three temperatures 298K, 308K and 318K, the results are shown in Table 3, the equation (13) represents the Arrhenius equation for calculating the activation energy  $E_a^*$  of the corrosion process [59,62,64], the values are calculated from the slope of the equation (13) the results found are shown in Table 9, while the lines are in Figure 8(left).

$$\log(C_r) = \log(A) - \frac{E_a^*}{2,303 \times R \times T} \quad (13)$$

Where  $C_r$  is the corrosion rate,  $R$  is the perfect gas constant,  $T$  is the temperature,  $A$  is the preexponential factor of Arrhenius.

Several authors calculating enthalpy of activation  $\Delta H_a^*$  and entropy of activation  $\Delta S_a^*$  [39]65], in order to verify the nature of the adsorption, these two parameters are calculated from the equation (14).

$$\log\left(\frac{C_r}{T}\right) = \log\left(\frac{R}{h \times N}\right) + \frac{\Delta S_a^*}{2,303 \times R} - \frac{\Delta H_a^*}{2,303 \times R \times T} \quad (14)$$

where  $h$  is Plank's constant,  $N$  is Avogadro's number.

The lines are shown in Figure 8(right), the enthalpy of activation was calculated from the intercept while the entropy of activation was calculated from the slope, the results presented in Table 9.

According to Table 9, the activation energy ( $E_a^*$ ) increases when the first two concentrations are added and then decreases with respect to that of the solution with sulfuric acid alone, it is shown in the literature that the increase of ( $E_a^*$ ) is synonymous with a physisorption [64,66], on the other hand, the decrease of this parameter implies a chemisorption [62,67,68], in our case we can assume that we have a mixture of the two types of adsorption since the activation energy barrier of the corrosion process decreases and increases for the OEE in the 0.5M H<sub>2</sub>SO<sub>4</sub> compared to that of the sulfuric acid alone, similar results were found by Yangyang Guo et al [69] for 1-vinyl-3-aminopropylimidazolium hexafluorophosphate in 1M HCl, Ali A.

Abd-Elaal et al [70] found the same things for Gemini quaternary G1000Br surfactants are activation energy at decreased compared to that of white at the concentration of  $5.10^{-5}M$ , Yangyang Guo et al [69] shows that 1-vinyl-3-aminopropylimidazolium hexafluorophosphate 1-vinyl-3-aminopropylimidazoliumtetrafluoroborate ([VAIM] [PF4]) is chemically adsorbed on carbon steel despite a high value compared to blank, in our study it can be assumed that there is both phenomenon during the adsorption of active species on the surface of C38 steel, this may explain the value obtained from the parameter b of the Adejo-Ekwenchi isotherm increases with increasing temperature. It is known in the literature that a positive value implies an endothermic phenomenon of the dissolution of metal [71,72], according to Moses M. Solomon et al [73] a value of  $\Delta H_a^*$  is lower than that of  $E_a^*$  which is in agreement with the formula:

$$E_a^* - \Delta H_a^* = R \times T \quad (15)$$

We also notice that we have large negative values of  $\Delta S_a^*$  the activated complex in the rate determining step is an association rather than dissociation step meaning that a decrease in disordering takes place on going from reactants to the activated complex [22,74,75].

According to Hassan Ramzi et al [16] found that essential oils of *Origanum elongatum* contained carvacrol (67.34% -81.72%),  $\gamma$ -terpinene (3.29%-10.75%), para-cymene (3.62%-7.81%) and thymol (1.79%-9.17%) are the majority compounds, and the study done by V. Vorobyova et al [76] who studied the inhibitory effect of carvacrol in 0.5 M  $Na_2SO_4$  for mild steel and found an efficacy of 99.87% at a concentration of 600mg/L.

**Table 1. Different parameters of linear polarization of the OEE in the  $H_2SO_4$  0.5M**

C (g/L)	$\beta_a$ (mV)	$\beta_c$ (mV)	$E_{corr}$ (mV/ESC)	$J_{corr}$ ( $\mu A/cm^2$ )	E %
0	23.6	41.6	-399.446	316.471	--
0.1	10.3	22.5	-368.842	98.682	68.82
0.2	25.2	77.9	-384.198	79.133	75.00
0.4	21.3	68.6	-376.374	75.816	76.04
0.8	25.0	61.5	-381.948	69.207	78.13
1	18.7	85.7	-365.607	56.426	82.17

**Table 2. Electrochemical parameters deduced by EIS method for mild steel C38 in 0.5M  $H_2SO_4$  in the absence and presence of various concentrations of OEE.**

C (g/L)	$R_s$ ( $\Omega$ )	$Q_{dl}.10^4$ ( $F.s^{n-1}$ )	n	$C_{dl}.10^4$ (F)	$R_{ct}$ ( $\Omega$ )	%E
Blank	1.383	5.78	0.883	3.17	18.42	--
0.1	1.492	2.05	0.898	1.22	50.54	63.55
0.2	1.558	2.26	0.888	1.31	58.51	68.52
0.4	1.645	2.06	0.889	1.19	60.00	69.30
0.8	1.518	2.42	0.889	1.43	61.28	69.94
1	3.286	1.73	0.902	1.06	67.47	72.70



**Table 3. Corrosion parameters obtained of mild steel C38 in 0.5M H<sub>2</sub>SO<sub>4</sub> solutions with and without addition of various concentrations of OEE.**

C (g/L)	Cr (g.cm <sup>-2</sup> .h <sup>-1</sup> ).10 <sup>3</sup>			%E		
	298 K	308 k	318 K	298 K	308 K	318 K
0	2.48	3.88	8.10	-	-	-
0.1	0.754	1.22	3.02	69.58	62.50	62.24
0.2	0.694	1.08	2.91	71.97	66.61	63.60
0.4	0.689	0.961	2.06	72.20	70.35	74.27
0.8	0.620	0.908	2.04	74.96	71.98	74.55
1	0.607	0.848	1.81	75.49	73.85	77.44

**Table 4. Different types of isotherm used for fitting results of OEE in 0.5M H<sub>2</sub>SO<sub>5</sub>**

Isotherms	Equation	Parametrs signification
Langmuir modified	$\frac{C}{\theta} = nC + \frac{n}{K_{ads}}$	n represents the slope [33].
Flory–Huggins	$\log\left(\frac{\theta}{C}\right) = \log(K_{ads}) + x \log(1-\theta)$	x is the number of active sites occupied by a single adsorbed molecule [34].
Frumkin	$\log\left\{C\left(\frac{\theta}{1-\theta}\right)\right\} = 2,303 \log K_{ads} + 2\alpha\theta$	α in this equation represents the interaction between the adsorbed species [35].
El-Awady	$\log\left(\frac{\theta}{1-\theta}\right) = \log K + y \log C$	The value of y gives information on the nature of the adsorbed layer, if y> 1 a multilayer is formed whereas if y<1 a monolayer [36].
Freundlich	$\log \theta = \log K_{ads} + n \log C$	n describes the ease with which the active species adsorb on the metal surface, generally it is known that a value of n between 0 and 1 the adsorption is easy while a value n ≥ 1 the adsorption is moderate or difficult [37].
Temkin	$\theta = \frac{-2,303 \log K_{ads}}{2a} - \frac{2,303 \log C}{2a}$	a gives an idea of the interaction within the adsorbed layer [38].
Adejo-Ekwenchi	$\log\left(\frac{1}{1-\theta}\right) = \log K_{ads} + b \log C$	b is the variation factor, it gives the link between the recovery rate and the concentration of the solution.[39]

**Table 5. Different isotherms and their parameters**

	T(K)	Slope	Intercept	R <sup>2</sup>	n	K <sub>ads</sub> (L/g)	ΔG <sup>0</sup> <sub>ads</sub> (kJ/mol)
Langmuir	298	1.310	0.018	0.9998	1.31	7.16.10 <sup>1</sup>	-27.70
	308	1.333	0.033	0.9997	1.33	4.09.10 <sup>1</sup>	-27.19
	318	1.258	0.046	0.9988	1.26	2.71.10 <sup>1</sup>	-26.99
Flory–Huggins					x		
	298	23.340	13.937	0.9419	23.34	8.65. 10 <sup>13</sup>	-96.63
	308	14.198	7.923	0.9817	14.20	8.38.10 <sup>7</sup>	-64.41
	318	8.022	4.975	0.8769	8.02	9.44.10 <sup>4</sup>	-48.55

					$\alpha$		
Frumkin	298	18.998	-13.847	0.9597	9.50	$9.71 \cdot 10^{-7}$	17.19
	308	11.105	-7.756	0.9854	5.55	$4.29 \cdot 10^{-4}$	2.17
	318	7.733	-5.600	0.9426	3.87	$4.09 \cdot 10^{-3}$	-3.73
					A		
Temkin	298	0.056	0.753	0.9489	-20.38	$2.14 \cdot 10^{13}$	-93.17
	308	0.108	0.738	0.9793	-10.69	$7.09 \cdot 10^6$	-58.08
	318	0.159	0.774	0.8988	-7.25	$7.47 \cdot 10^4$	-47.93
					$1/y$		
El-Awady	298	0.124	0.484	0.9470	8.08	$8.16 \cdot 10^3$	-39.43
	308	0.217	0.447	0.9826	4.60	$1.14 \cdot 10^2$	-29.82
	318	0.329	0.529	0.9001	3.04	$4.03 \cdot 10^1$	-28.04
					n		
Freundlich	298	0.034	-0.123	0.9497	0.04	$7.53 \cdot 10^{-1}$	-16.41
	308	0.069	-0.131	0.9752	0.07	$7.39 \cdot 10^{-1}$	-16.91
	318	0.100	-0.110	0.8982	0.10	$7.76 \cdot 10^{-1}$	-17.59
					b		
Adejo-Ekwenchi	298	0.090	0.6069	0.9455	0.09	1.23	-17.63
	308	0.148	0.5782	0.9844	0.15	1.41	-18.57
	318	0.230	0.6393	0.8999	0.23	1.70	-19.66

 Table 6.  $R_L$  Values for Langmuir Isotherm for All Temperatures

C (g/L)	Langmuir		
	298K	308K	318K
0.1	0.123	0.197	0.269
0.2	0.065	0.109	0.156
0.4	0.034	0.058	0.084
0.8	0.017	0.030	0.044
1	0.014	0.024	0.036

Table 7. Free energy of adsorption, enthalpy of adsorption and entropy energy of adsorption of the OEE.

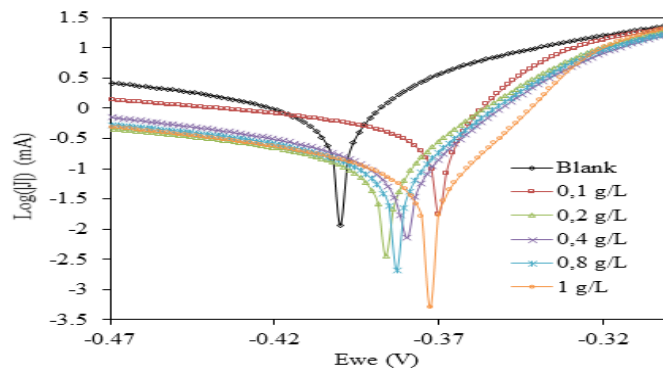
T (K)	$\Delta G_{ads}^0$ (kJ/mol)	$\Delta H_{ads}^0$ (kJ/mol)	$\Delta S_{ads}^0$ (J/mol. K)
298	-27.70		-35.22
308	-27.19	-38.195	-35.73
318	-26.99		-35.24

Table 8. Dubinin-Radushkevich parameters

T (K)	R <sup>2</sup>	a (mol <sup>2</sup> /KJ)	E (kJ/mol)
298	0.8854	0.0232	4.6424
308	0.9822	0.0459	3.3005
318	0.8657	0.0611	2.8606

**Table 9. Activation parameters of the dissolution of C38 in 0.5M H<sub>2</sub>SO<sub>4</sub> in the absence and presence of various concentrations of OEE.**

C (g/L)	$\Delta H_a^*$ (kJ/mol)	$\Delta S_a^*$ (J/mol.K)	$E_a^*$ (kJ/mol)	A (g.m <sup>-2</sup> .h <sup>-1</sup> )	$E_a^* - \Delta H_a^*$ (kJ/mol)
0	43.50	-149.29	46.06	2.78.10 <sup>5</sup>	2.5582
0.1	51.96	-131.05	54.52	2.50.10 <sup>6</sup>	2.5601
0.2	53.68	-126.09	56.24	4.54.10 <sup>6</sup>	2.5601
0.4	40.39	-170.59	42.95	2.15.10 <sup>4</sup>	2.5601
0.8	44.09	-159.05	46.65	8.62.10 <sup>4</sup>	2.5582
1	40.17	-172.36	42.73	1.74.10 <sup>4</sup>	2.5601



**Figure 1 Polarization curves of the OEE in H<sub>2</sub>SO<sub>4</sub> 0.5M on C38 steel.**

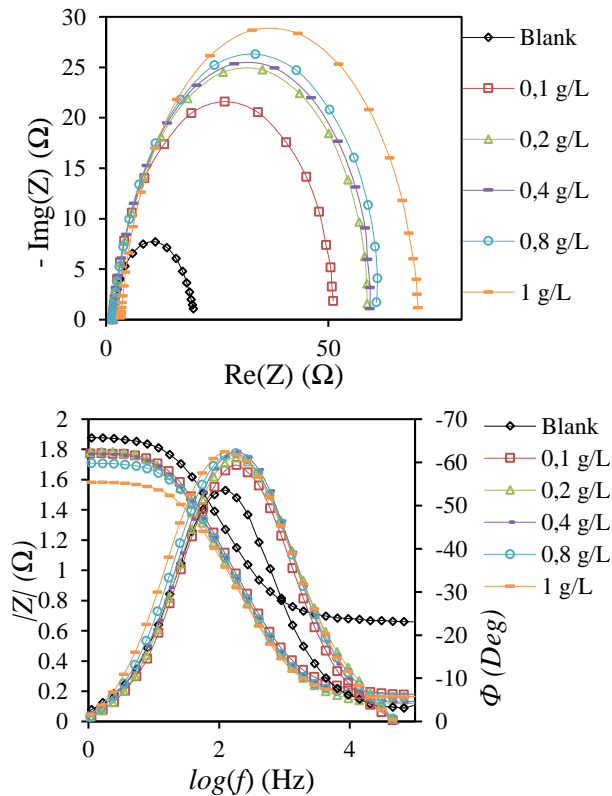


**Figure 2 EIS (left) bode diagrams (right) for mild steel C38 in 0.5M H<sub>2</sub>SO<sub>4</sub> with different concentrations of OEE at 298K.**

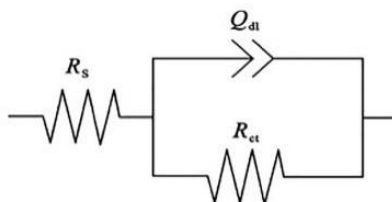


Figure 3 Equivalent circuit used to fit the experimental result.

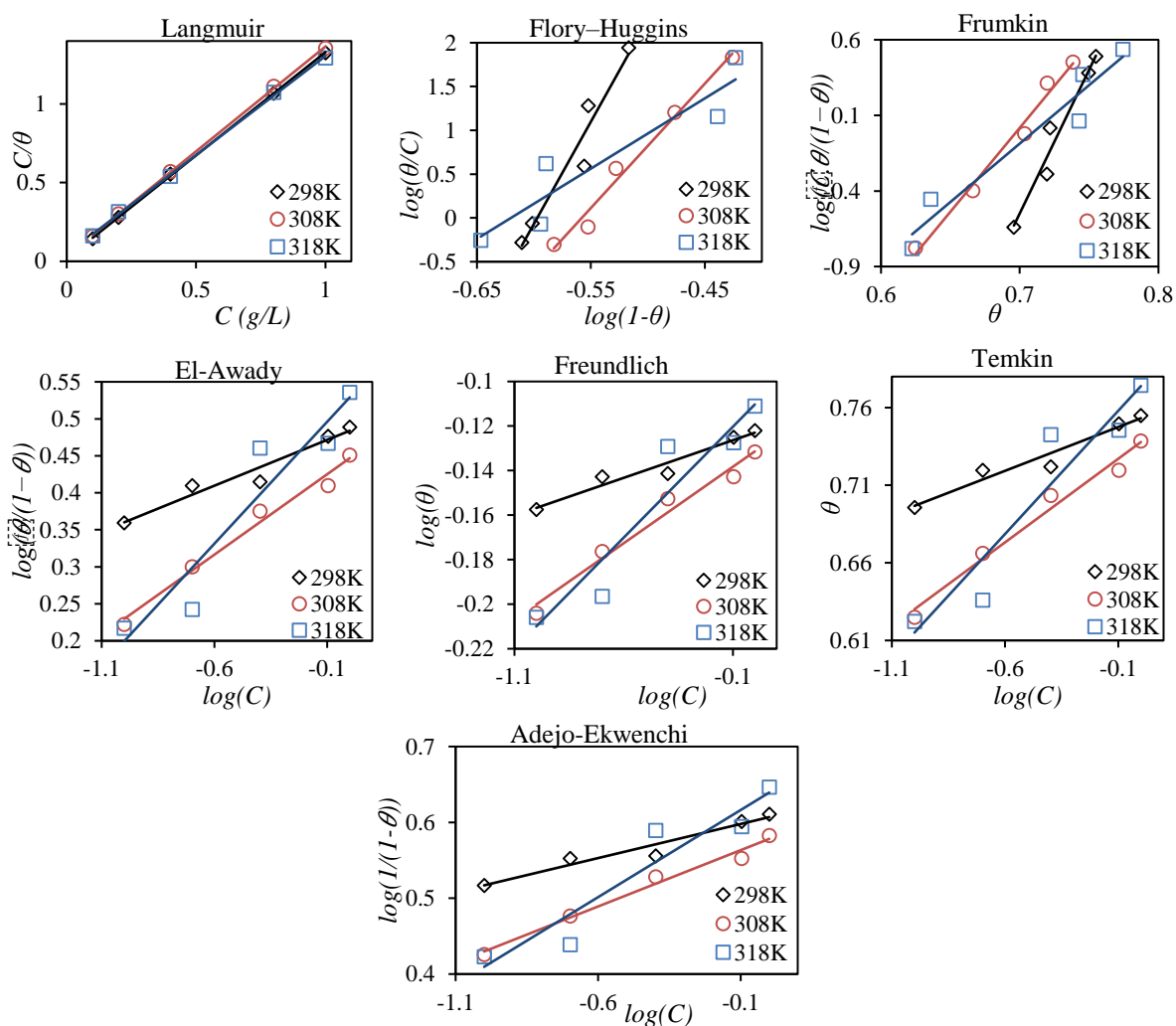


Figure 3 Isotherms used to choose the one from which we will make the kinetic calculations.

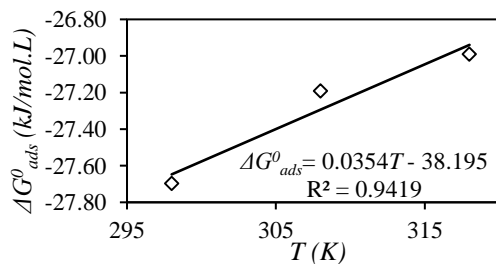


Figure 4 Thermodynamic parameters for the adsorption of OEE onto the mild steel surface in 0.5M H<sub>2</sub>SO<sub>4</sub>.

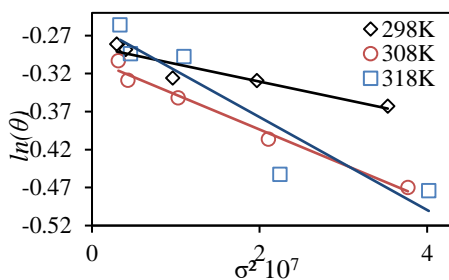


Figure 5 Dubinin-Radushkevich isotherm for OEE.

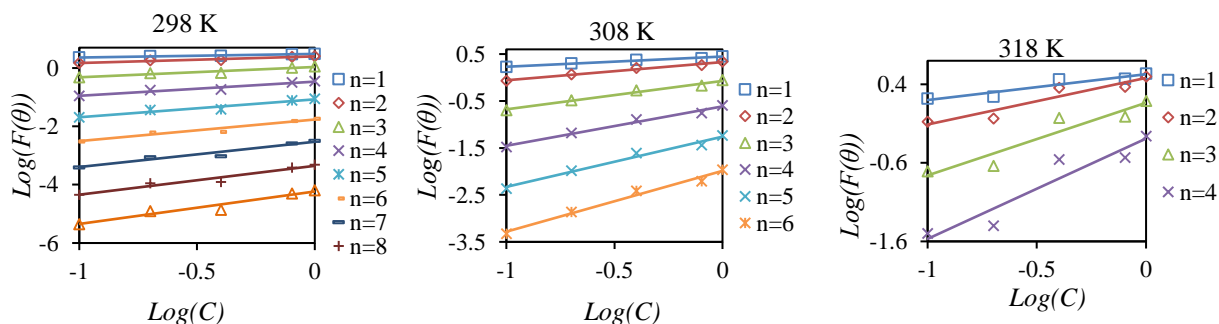


Figure 6 Bockris-Swinkels isotherm in different temperatures for the OEE in 0,5M H<sub>2</sub>SO<sub>4</sub>

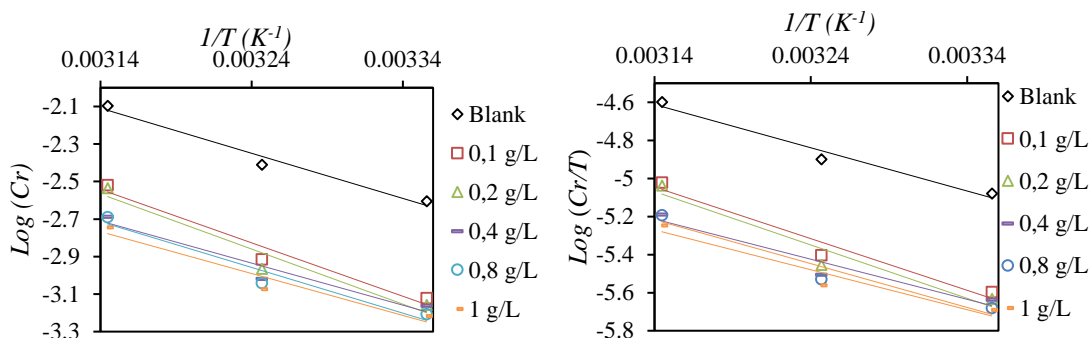


Figure 7(left) Arrhenius plots of  $\log(Cr)$  versus  $1/T$ , (right) and  $\log(Cr/T)$  versus  $1/T$  in the absence and presence of different concentrations of OEE in 0.5M H<sub>2</sub>SO<sub>4</sub>.

### CONCLUSION

- (1) Electrochemical tests show that; according to the linear polarization the extract acts as a mixed inhibitor with an anodic tendency, electrochemical impedance spectroscopy shows that the active species of the extract act by adsorption on the metal surface with an increase in the thickness of the adsorbing layer as the concentration of the extract increases.
- (2) The fitting of the results by several isotherms shows that the Langmuir isotherm is the best adapted for this study, despite the fact that all the isotherms have a correlation coefficient  $R^2$  close to 1.
- (3) Thermodynamic calculations show that there is a mixture of physisorption and chemisorption between the active species of the extract and the metal surface.
- (4) The kinetic study concludes that the metal dissolution is endothermic.

### REFERENCES

- [1] Li X, Xie X. Adsorption and inhibition effect of two aminopyrimidine derivatives on steel surface in

- H<sub>2</sub>SO<sub>4</sub> solution. J Taiwan Inst Chem Eng. 2014;45(6):3033-3045. doi:10.1016/j.jtice.2014.08.019.
- [2] Daoud D, Douadi T, Issaadi S, et al. Adsorption and corrosion inhibition of new synthesized thiophene Schiff base on mild steel X52 in HCl and H<sub>2</sub>SO<sub>4</sub> solutions. Corros Sci. 2014;79:50-58. doi:10.1016/j.corsci.2013.10.025.
- [3] Deng S, Li X, Fu H. Alizarin violet 3B as a novel corrosion inhibitor for steel in HCl, H<sub>2</sub>SO<sub>4</sub> solutions. Corros Sci. 2011;53(11):3596-3602. doi:10.1016/j.corsci.2011.07.003.
- [4] Guo L, Zhu S, Zhang S. Experimental and theoretical studies of benzalkonium chloride as an inhibitor for carbon steel corrosion in sulfuric acid. J Ind Eng Chem. 2015;24:174-180. doi:10.1016/j.jiec.2014.09.026.
- [5] Obot IB, Umoren SA, Obi-egbedi NO. Corrosion inhibition and adsorption behaviour for aluminum by extract of *Aningeria robusta* in HCl solution : Synergistic effect of iodide ions. 2011;2(1):60-71.
- [6] Kardas G, Yazıcı B. Electrochemical and quantum chemical studies of 2-amino-4-methyl-thiazole as corrosion inhibitor for mild steel in HCl solution. 2014;83:310-316. doi:10.1016/j.corsci.2014.02.029.
- [7] Boumhara K, Tabyaoui M, Jama C, et al. *Artemisia Mesatlantica* essential oil as green inhibitor for carbon steel corrosion in 1 M HCl solution: Electrochemical and XPS investigations. J Ind Eng Chem. 2015;29:146-155. doi:10.1016/j.jiec.2015.03.028.
- [8] Singh AK, Mohapatra S, Pani B. Corrosion inhibition effect of *Aloe Vera* gel: Gravimetric and electrochemical study. J Ind Eng Chem. 2016;33:288-297. doi:10.1016/j.jiec.2015.10.014.
- [9] Soltani N, Tavakkoli N, Kashani MK, et al. *Silybum marianum* extract as a natural source inhibitor for 304 stainless steel corrosion in 1.0 M HCl. J Ind Eng Chem. 2014;20(5):3217-3227. doi:10.1016/j.jiec.2013.12.002.
- [10] Olusegun J, Akintoye C, Idowu AP. *Rhizophora mangle L.* effects on steel-reinforced concrete in 0.5 M H<sub>2</sub>SO<sub>4</sub> : Implications for corrosion-degradation of wind-energy structures in industrial environments. Energy Procedia. 2014;50:429-436. doi:10.1016/j.egypro.2014.06.052.
- [11] El Bribri A, Tabyaoui M, Tabyaoui B, et al. The use of *Euphorbia falcata* extract as eco-friendly corrosion inhibitor of carbon steel in hydrochloric acid solution. Mater Chem Phys. 2013;141(1):240-247. doi:10.1016/j.matchemphys.2013.05.006.
- [12] Faustin M, Maciuk A, Salvin P, et al. Corrosion inhibition of C38 steel by alkaloids extract of *Geissospermum laeve* in 1M hydrochloric acid : electrochemical and phytochemical studies. Corros Sci. 2014. doi:10.1016/j.corsci.2014.12.005.
- [13] Bammou L, Belkhaouda M, Salghi R, et al. Corrosion inhibition of steel in sulfuric acidic solution by the *Chenopodium Ambrosioides* extracts. J Assoc Arab Univ Basic Appl Sci. 2014;16:83-90. doi:10.1016/j.jaubas.2013.11.001.
- [14] Prabakaran M, Kim SH, Hemapriya V, et al. Evaluation of polyphenol composition and anti-corrosion properties of *Cryptostegia grandiflora* plant extract on mild steel in acidic medium. J Ind Eng Chem. 2016;37:47-56. doi:10.1016/j.jiec.2016.03.006.
- [15] Umoren SA, Eduok UM, Solomon MM, et al. Corrosion inhibition by leaves and stem extracts of *Sida acuta* for mild steel in 1 M H<sub>2</sub>SO<sub>4</sub> solutions investigated by chemical and spectroscopic techniques. Arab J Chem. 2016;9:S209-S224. doi:10.1016/j.arabjc.2011.03.008.
- [16] Ramzi H, Ismaili MR, Aberchane M, et al. Chemical characterization and acaricidal activity of *Thymus satureioides* C. & B. and *Origanum elongatum* E. & M. (Lamiaceae) essential oils against *Varroa destructor* Anderson & Trueman (Acari: Varroidae). Ind Crops Prod. 2017;108(June):201-207. doi:10.1016/j.indcrop.2017.06.031.
- [17] Khadiri A, Saddik R, Bekkouche K, et al. Gravimetric, electrochemical and quantum chemical studies of some pyridazine derivatives as corrosion inhibitors for mild steel in 1M HCl solution. J Taiwan Inst Chem Eng. 2015;58:552-564. doi:10.1016/j.jtice.2015.06.031.
- [18] Yadav M, Gope L, Kumari N, et al. Corrosion inhibition performance of pyranopyrazole derivatives for mild steel in HCl solution : Gravimetric , electrochemical and DFT studies. J Mol Liq. 2016;216:78-86. doi:10.1016/j.molliq.2015.12.106.
- [19] Li X, Deng S, Fu H. Synergistic inhibition effect of 6-benzylaminopurine and iodide ion on the corrosion of cold rolled steel in H<sub>3</sub>PO<sub>4</sub> solution. Corros Sci. 2011;53(11):3704-3711. doi:10.1016/j.corsci.2011.07.016.
- [20] Li X, Deng S, Fu H. *Allyl thiourea* as a corrosion inhibitor for cold rolled steel in H<sub>3</sub>PO<sub>4</sub> solution. Corros Sci. 2012;55:280-288. doi:10.1016/j.corsci.2011.10.025.
- [21] Hegazy MA, Aiad I. Bromide as a novel corrosion inhibitor for carbon steel during phosphoric acid production. J Ind Eng Chem. 2015;31:91-99. doi:10.1016/j.jiec.2015.06.012.
- [22] Soltani N, Tavakkoli N, Khayatkashani M, et al. Green approach to corrosion inhibition of 304 stainless

- steel in hydrochloric acid solution by the extract of *Salvia officinalis* leaves. Corros Sci. 2012;62:122-135. doi:10.1016/j.corsci.2012.05.003.
- [23] Li X, Deng S, Fu H. Triazolyl blue tetrazolium bromide as a novel corrosion inhibitor for steel in HCl and H<sub>2</sub>SO<sub>4</sub> solutions. Corros Sci. 2011;53(1):302-309. doi:10.1016/j.corsci.2010.09.036.
- [24] Hegazy MA, Atlam FM. Three novel bolaamphiphiles as corrosion inhibitors for carbon steel in hydrochloric acid: Experimental and computational studies. J Mol Liq. 2016;218:649-662. doi:10.1016/j.molliq.2016.03.008.
- [25] Hegazy MA, Aiad I. 1-Dodecyl-4-((3-morpholinopropyl)imino)methylpyridin-1-ium bromide as a novel corrosion inhibitor for carbon steel during phosphoric acid production. J Ind Eng Chem. 2015;31:91-99. doi:10.1016/j.jiec.2015.06.012.
- [26] Verma CB, Quraishi MA, Singh A. 2-Aminobenzene-1,3-dicarbonitriles as green corrosion inhibitor for mild steel in 1 M HCl: Electrochemical, thermodynamic, surface and quantum chemical investigation. J Taiwan Inst Chem Eng. 2015;49:229-239. doi:10.1016/j.jtice.2014.11.029.
- [27] Benabbouha T, Siniti M, El Attari H, et al. Red Algae *Halopitys Incurvus* Extract as a Green Corrosion Inhibitor of Carbon Steel in Hydrochloric Acid. J Bio- Tribo-Corrosion. 2018;4(39). doi:10.1007/s40735-018-0161-0.
- [28] Zhang QB, Hua YX. Corrosion inhibition of mild steel by alkylimidazolium ionic liquids in hydrochloric acid. Electrochim Acta. 2009;54(6):1881-1887. doi:10.1016/j.electacta.2008.10.025.
- [29] Yadav M, Sharma U, Yadav P. Corrosion inhibitive properties of some new isatin derivatives on corrosion of N80 steel in 15 % HCl. Int J Ind Chem. 2013:1-10.
- [30] El Rehim SSA, Sayyah SM, El-Deeb MM, et al. Adsorption and corrosion inhibitive properties of P( 2-aminobenzothiazole ) on mild steel in hydrochloric acid media. Int J Ind Chem. 2016;7(1):39-52. doi:10.1007/s40090-015-0065-5.
- [31] John S, Jeevana R, Aravindakshan K.K, et al. Corrosion inhibition of mild steel byN(4)-substituted thiosemicarbazone in hydrochloric acid media. Egypt J Pet. 2017;(26): 405-412. doi:10.1016/j.ejpe.2016.05.012
- [32] El Attari H, Chefira K, Siniti M, et al. Adsorption and Corrosion Inhibition Performance of 1,3-Dihydro-2H- benzimidazole-2-thione for Mild Steel C35E in Sulfuric Acid Solution. Int J Recent Trends Eng Res. 2017;3(1):167-179.
- [33] M. Sundaravadivelu, Karthik G, Vengatesh G. A comprehensive study of ondansetron hydrochloride drug as a green corrosion inhibitor for mild steel in 1 M HCl medium A comprehensive study of ondansetron hydrochloride drug as a green corrosion inhibitor for mild steel in 1 M HCl medium. Egypt J Pet. 2016;(November):1-15. doi:10.1016/j.ejpe.2016.10.011.
- [34] Adejo SO, Ekwenchi MM, Olatunde PO, et al. Adsorption characteristics of ethanol root extract of *Portulaca oleracea* as eco-friendly inhibitor of corrosion of mild steel in H<sub>2</sub>SO<sub>4</sub> medium. J Appl Chem. 2014;(4):55-60.
- [35] Adejo SO, Ekwenchi MM, Momoh F, et al. Adsorption Characterization of Ethanol Extract of Leaves of *Portulaca oleracea* as Green Corrosion Inhibitor for Corrosion of Mild Steel in Sulphuric Acid Medium. Int J Mod Chem. 2015;(3):125-134. doi:10.9790/5736-07415560.
- [36] Emran KM, Ahmed NM, Torjoman BA, et al. *Cantaloupe* Extracts as Eco Friendly Corrosion Inhibitors for Aluminum in acidic and alkaline solutions. J Mater Environ Sci. 2014;5(6):1940-1950.
- [37] Ahile UJ, Adejo SO, Gbertyo JA, et al. Ethanol Stem Extract Of *Mucuna Pruriens* As Green Corrosion Inhibitor For Corrosion of Aluminium In H<sub>2</sub>SO<sub>4</sub>. J Appl Chem. 2014;3 (5):(5):2039-2046.
- [38] Okeniyi JO. C<sub>10</sub>H<sub>18</sub>N<sub>2</sub>Na<sub>2</sub>O<sub>10</sub> inhibition and adsorption mechanism on concrete steel-reinforcement corrosion in corrosive environments. J Assoc Arab Univ Basic Appl Sci. 2016;20:39-48. doi:10.1016/j.jaubas.2014.08.004.
- [39] Shukla SK, Ebenso EE. Corrosion inhibition, adsorption behavior and thermodynamic properties of streptomycin on mild steel in hydrochloric acid medium. Int J Electrochem Sci. 2011;6(8):3277-3291.
- [40] Ahile UJ, Gbertyo JA, Anzene JS, et al. Evaluation Of The Inhibitive Properties And Adsorptive Parameters Of Ethanol Leaf Extract Of *Mucuna Pruriens* For The Corrosion Inhibition Of Aluminium In 2 M H<sub>2</sub>SO<sub>4</sub> Solution. Int. j. innov. sci. eng. technol. 2014;1(6):176-185.
- [41] Eddy NO, Ita BI, Ibisi NE, et al. Experimental and Quantum Chemical Studies on the Corrosion Inhibition Potentials of 2-(2-Oxoindolin-3-Ylideneamino) Acetic Acid and Indoline-2,3-Dione. Int J Electrochem Sci. 2011;6:1027-1044.
- [42] Nwabanne JT, Okafor VN. Adsorption and Thermodynamics Study of the Inhibition of Corrosion of Mild Steel in H<sub>2</sub>SO<sub>4</sub> Medium Using *Vernonia amygdalina*. J Miner Mater Charact Eng. 2012;11:885-890.
- [43] Yaro AS, Khadom AA, Wael RK. Apricot juice as green corrosion inhibitor of mild steel in phosphoric

- acid. Alexandria Eng J. 2013;52(1):129-135. doi:10.1016/j.aej.2012.11.001.
- [44] Zheng H, Liu D, Zheng Y, et al. Sorption isotherm and kinetic modeling of aniline on Cr-bentonite. J Hazard Mater. 2009;167(1-3):141-147. doi:10.1016/j.jhazmat.2008.12.093.
- [45] Adejo SO, Yiase SG, Ahile UJ, et al. Inhibitory effect and adsorption parameters of extract of leaves of *Portulaca oleracea* of corrosion of aluminium in H<sub>2</sub>SO<sub>4</sub> solution. Sch Res Libr Arch. 2013;5(1):25-32.
- [46] Ouici H, Tourabi M, Benali O, et al. Experimental investigation on the corrosion inhibition characteristics of mild steel by 5-(2-hydroxyphenyl)-1,3,4-oxadiazole-2-thiol in hydrochloric acid medium. J Mater Environ Sci. 2016;7(8):2971-2988.
- [47] Khadom AA, Yaro AS, Altaie AS, et al. Activations and Adsorption Studies for the Corrosion Inhibition of Low Carbon Steel in Acidic Media. Port Electrochim Acta. 2009;27(6):699-712. doi:10.4152/pea.200906699.
- [48] El Attari H, Mengouch S, Siniti M, et al. Corrosion Inhibition Behaviour and Adsorption Characteristics of Quinoxaline Derived on Mild Steel C38E in Acid Medium. Int J Innov Res Sci Eng Technol. 2017;6(1):1-16. doi:10.9734/ACSj/2015/18211.
- [49] Ben Hmamou D, Salghi R, Zarrok H, et al. Temperature Effects on the Corrosion Inhibition of Carbon Steel in Acidic Solutions by Alizarin Red. Adv Mater Corros. 2012;2:36-42.
- [50] Kshama Shetty S, Nityananda Shetty A. Eco-friendly benzimidazolium based ionic liquid as a corrosion inhibitor for aluminum alloy composite in acidic media. J Mol Liq. 2017;225:426-438. doi:10.1016/j.molliq.2016.11.037.
- [51] Murulana LC, Kabanda MM, Ebenso EE. Investigation of the adsorption characteristics of some selected sulphonamide derivatives as corrosion inhibitors at mild steel/hydrochloric acid interface: Experimental, quantum chemical and QSAR studies. J Mol Liq. 2016;215:763-779. doi:10.1016/j.molliq.2015.12.095.
- [52] Hammouti B, Zarrouk A, Al-deyab SS, et al. Temperature Effect, Activation Energies and Thermodynamics of Adsorption of ethyl 2-(4-(2-ethoxy-2-oxoethyl)-2-p-Tolylquinoxalin-1 (4H)-yl) Acetate on Cu in. Orient J Chem. 2011;27(1):23-31. <http://www.orientjchem.org/dnload/B-Hammouti-A-Zarrouk-SS-AlDeyab-and-I-Warad/OJCV027I01P23-31.pdf>.
- [53] Ezeoke AU, Obi-Egbedi NO, Adeosun CB, et al. Synergistic Effect of Leaf Extracts of *Cordia sebestena* L. and Iodide Ions on the Corrosion Inhibition of Mild Steel in Sulphuric Acid. Int J Electrochem Sci. 2012;7:5339-5355.
- [54] Obot IB, Obi-egbedi NO. Anti-corrosive properties of xanthone on mild steel corrosion in sulphuric acid: Experimental and theoretical investigations. Curr Appl Phys. 2011;11(3):382-392. doi:10.1016/j.cap.2010.08.007.
- [55] Obot IB, Obi-egbedi NO, Umoren SA, et al. Adsorption and Kinetic Studies on the Inhibition Potential of Fluconazole for the Corrosion of Al in HCl Solution. Chem Eng Commun. 2011;(198):711-725. doi:10.1080/00986445.2011.532746.
- [56] Gemeay AH, El-Sherbiny AS, Zaki AB. Adsorption and Kinetic Studies of the Intercalation of Some Organic Compounds onto Na<sup>+</sup>-Montmorillonite. J Colloid Interface Sci. 2002;(245):116-125. doi:10.1006/jcis.2001.7989.
- [57] Caliskan N, Akbas E. Corrosion inhibition of austenitic stainless steel by some pyrimidine compounds in hydrochloric acid. Mater Corros. 2012;63(3):231-237. doi:10.1002/maco.201005788.
- [58] Solomon MM, Umoren SA, Udoso II, et al. Inhibitive and adsorption behaviour of carboxymethyl cellulose on mild steel corrosion in sulphuric acid solution. Corros Sci. 2010;52(4):1317-1325. doi:10.1016/j.corsci.2009.11.041.
- [59] Ating EI, Umoren SA, Udoso II, et al. Leaves extract of *Ananas sativum* as green corrosion inhibitor for aluminium in hydrochloric acid solutions. Green Chem Lett Rev. 2010;3(2):61-68. doi:10.1080/17518250903505253.
- [60] Fouda AS, Madkour LH, El-Shafei AA, et al. Corrosion inhibitors for zinc in 2M HCl solution. Bull Korean Chem Soc. 1995;16(5):454-458.
- [61] Saleh MM, Atia AA. Effects of structure of the ionic head of cationic surfactant on its inhibition of acid corrosion of mild steel. J Appl Electrochem. 2006;36:899-905. doi:10.1007/s10800-006-9147-6.
- [62] Abdul Rahiman AFS, Sethumanickam S. Corrosion inhibition, adsorption and thermodynamic properties of poly(vinyl alcohol-cysteine) in molar HCl. Arab J Chem. 2017;10:S3358-S3366. doi:10.1016/j.arabjc.2014.01.016.
- [63] Fouda AS, Al-sarawy AA, Ahmed FS, et al. Corrosion inhibition of aluminum 6063 using some pharmaceutical compounds. Corros Sci. 2009;51(3):485-492. doi:10.1016/j.corsci.2008.10.012.
- [64] Singh DK, Kumar S, Udayabhanu G, et al. 4(N,N-dimethylamino) benzaldehyde nicotinic hydrazone as



- corrosion inhibitor for mild steel in 1M HCl solution: An experimental and theoretical study. *J Mol Liq.* 2016;216:738-746. doi:10.1016/j.molliq.2016.02.012.
- [65] Ouici H, Tourabi M, Benali O, et al. Adsorption and corrosion inhibition properties of 5-amino 1,3,4-thiadiazole-2-thiol on the mild steel in hydrochloric acid medium: Thermodynamic, surface and electrochemical studies. *J Electroanal Chem.* 2017;803(September):125-134. doi:10.1016/j.jelechem.2017.09.018.
- [66] Ansari KR, Quraishi MA, Singh A. Pyridine derivatives as corrosion inhibitors for N80 steel in 15 % HCl : Electrochemical , surface and quantum chemical studies. *MEASUREMENT.* 2015;76:136-147. doi:10.1016/j.measurement.2015.08.028.
- [67] Negm NA, Zaki MF. Physicochemical and Engineering Aspects Corrosion inhibition efficiency of nonionic Schiff base amphiphiles of p-aminobenzoic acid for aluminum in 4N HCl. *Colloids Surfaces A Physicochem Eng Asp.* 2008;322:97-102. doi:10.1016/j.colsurfa.2008.02.027.
- [68] Akalezi CO, Enenebaku CK, Oguzie EE. Application of aqueous extracts of *coffee senna* for control of mild steel corrosion in acidic environments. *Int J Ind Chem.* 2012;3(1):3-14.
- [69] Guo Y, Xu B, Liu Y, et al. Corrosion inhibition properties of two imidazolium ionic liquids with hydrophilic tetrafluoroborate and hydrophobic hexafluorophosphate anions in acid medium. *J Ind Eng Chem.* 2017;56:234-247. doi:10.1016/j.jiec.2017.07.016.
- [70] Abd-Elal AA, Shaban SM, Tawfik SM. Three Gemini cationic surfactants based on polyethylene glycol as effective corrosion inhibitor for mild steel in acidic environment. *J Assoc Arab Univ Basic Appl Sci.* 2017. doi:10.1016/j.jaubas.2017.03.004.
- [71] Abdallah M, AlTass HM, Al Jahdaly BA, et al. Inhibition properties and adsorption behavior of 5-arylazothiazole derivatives on 1018 carbon steel in 0.5 M H<sub>2</sub>SO<sub>4</sub> solution. *J Mol Liq.* 2016;216:590-597. doi:10.1016/j.molliq.2016.01.077.
- [72] Muthukrishnan P, Jeyaprabha B, Prakash P. Adsorption and corrosion inhibiting behavior of *Lannea coromandelica* leaf extract on mild steel corrosion. *Arab J Chem.* 2017;10:S2343-S2354. doi:10.1016/j.arabjc.2013.08.011.
- [73] Solomon MM, Gerengi H, Kaya T, et al. Enhanced corrosion inhibition effect of chitosan for St37 in 15% H<sub>2</sub>SO<sub>4</sub> environment by silver nanoparticles. *Int J Biol Macromol.* 2017;104:638-649. doi:10.1016/j.ijbiomac.2017.06.072.
- [74] Prabhu D, Rao P. *Coriandrum sativum* L. A novel green inhibitor for the corrosion inhibition of aluminium in 1.0M phosphoric acid solution. *J Environ Chem Eng.* 2013;1(4):676-683. doi:10.1016/j.jece.2013.07.004.
- [75] Abdallah M, Sobhi M, AlTass HM. Corrosion inhibition of aluminum in hydrochloric acid by pyrazinamide derivatives. *J Mol Liq.* 2016;223:1143-1150. doi:10.1016/j.molliq.2016.09.006.
- [76] Vorobyova V, Chygyrynets O, Skiba M, et al. Self-assembled monoterpene phenol as vapor phase atmospheric corrosion inhibitor of carbon steel. *Int J Corros Scale Inhib.* 2017;6(4):485-503. doi:10.17675/2305-6894-2017-6-4-8.